Measurement of Magnetic Properties of Soft Magnetic Composite Material (SOMALOY 700) by Using 3-D Magnetic Tester

A. R. Asari, Youguang Guo, and Jianguo Zhu
Faculty of Engineering and Information Technology, University of Technology Sydney
81 Broadway, Ultimo, NSW 2007, Australia

***Abstract* — Core loss for rotating electrical machine can be predicted by identifying the magnetic properties of the particular magnetic material. The magnetic properties should be properly measured since there are some variations of vector flux density in the rotating machine. In this paper, a kind of soft magnetic composite material, SOMALOY 700, has been measured under one axis flux density penetration by using a 3-D magnetic tester. The LabVIEW has been used to measure the induced voltages of B (magnetic flux density) and H (magnetic field strength) sensing coils. The voltages are used in obtaining the magnetic properties of the sample such as B, H, hysteresis loop and core loss by using the Mathcad software.**

***Index Terms* — core loss, hysteresis loop, SOMALOY 700 material, 3-D magnetic tester.**

I. Introduction

Soft magnetic materials have been used in various electrical appliances at various operating frequencies for more than 100 years. The unique soft magnetic composite (SMC) materials are developed to support the needs of advanced electrical motor applications with complex structure and 3-D magnetic flux path [1]. To properly design and analyze these machines, the 3-D magnetic properties should be obtained and understood. Several kinds of SMC material have been measured and analyzed by using a 3-D magnetic property tester [2-18].

The 3-D magnetic property tester was successfully developed by Zhu *et al.* in 2001 in order to investigate the magnetic properties of soft magnetic materials under 3-D magnetic excitations [2]. This system consists of a 3-D yoke to guide the magnetic fluxes in three axes, a data acquisition system, and three groups of coils to produce magnetic field along the orthogonal *x*-, *y*- and *z*- axes. The tester is able to produce different magnetic flux patterns such as alternating, rotating in a plane and rotating in a 3-D pattern.

In this paper, the magnetic properties of SOMALOY 700 (5P), a type of SMC material, are investigated by using the 3-D magnetic tester, as shown in Fig. 1. Fig. 2 shows the cubic SMC sample with length of 20 mm, together with the H and B sensing coils. Six guarding pieces of 20 x 20 x 6 mm^3 are used in this measurement for improving the uniformity of flux density within the sample. The guarding piece is made of the same material as the test specimen [3] as shown in Fig. 3. The magnetic properties of the sample under the *x*-axis penetration of 50 Hz frequency are reported in this paper.

The sensing coils are important subject to be focused. Therefore, the structure of both B and H coils should be well formed. The 200 turns of H sensing coil is wound around 0.6 mm thickness epoxy resin board. The round B sensing coil with 6 mm diameter has been embedded in the center of the H coil and it has been wound for 60 turns as shown in Fig. 4.

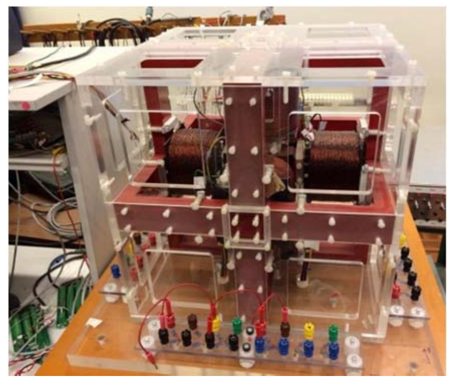

Fig. 1. 3-D magnetic property tester.

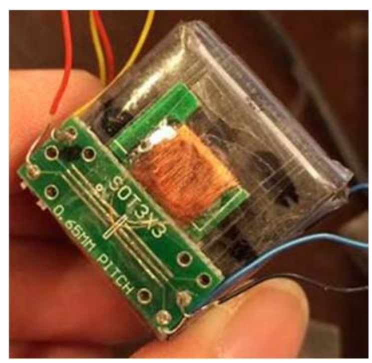

Fig. 2. Cubic SMC sample with sensing coils.

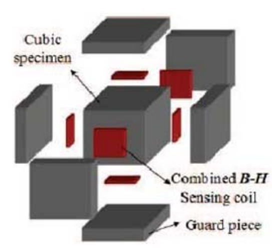

Fig. 3. Structure of guarding pieces: cubic sensing box with sample, sensing coils and guard piece [3].

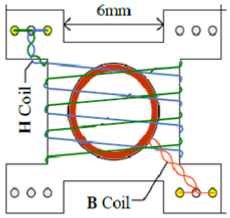

Fig. 4. Structure of B and H sensing coils [4].

In Fig. 5, each 16-layer excitation winding includes three coils, 2-layer coil for No. 1, 6-layer coil for No. 2, and 8-layer coil for No. 3, and each layer is designed to be 35 turns [5]. No.1 coil is for 200-1000 Hz, No. 1 and No. 2 coils are assigned for 20-200 Hz experiment, and all the three coils of No. 1, No. 2 and No. 3 are set to be in series for 2-20 Hz experiment as displayed in Fig. 6 [6].

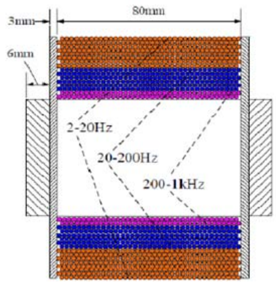

Fig. 5. Scheme of improved excitation winding coil [5].

Each pair of excitation winding coils are connected in series or parallel depending on the required frequency and impedance. Thus, both low and high frequency can be detected since each level of frequency has been assigned for the particular excitation coils. Fig. 6 illustrates the scheme of excitation and sensing structure in the x axis. It is also applied in the y and z axes. Experiment implementation for different typical frequency scope is performed by selecting the option switch of corresponding excitation coil [6]. The two exciting winding coils of x axis are connected in series without phase angle difference to ensure the generation of maximum and uniform magnetic field inside the sample [6, 18].

From the scheme of excitation and sensing structure, it can be seen that the operational amplifier (OA) is needed before data acquisition since the voltage of H signal is very small [6]. The actual figure of operational amplifiers is shown in Fig. 7.

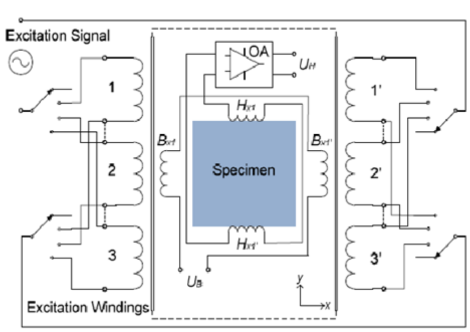

Fig. 6. Excitation and sensing structure in one axis [6].

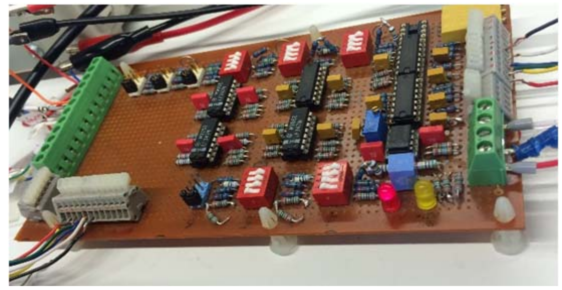

Fig. 7. Set of operational amplifiers for V_B and V_H signals.

II. Calibration of Sensing Coils

The sample surface field intensity components and the flux density components can be detected by B (magnetic flux density) and H (magnetic field strength) sensing coils which induce the sensing voltages.

The B and H can be obtained by

$$B = \frac{1}{K_B} \int V_B dt \tag{1}$$

$$H = \frac{1}{\mu_0 K_H} \int V_H dt \tag{2}$$

where V is the RMS value of the induced EMF, K_H is the coefficient for H coil and K_B is the coefficient for B coil .

The coil coefficients (in m^2) can be obtained by conducting a calibration in a long solenoid. Calibration of sensing coil was studied by considering the following equations [19-20].

$$K_H = \frac{V_H}{\sqrt{2}\pi f \mu_0 H_m} \tag{3}$$

$$K_B = \frac{V_B}{\sqrt{2}\pi f \mu_0 H_m} \tag{4}$$

where f is the frequency of the excitation current, and H_m is the magnitude of the magnetic field strength in the center of the solenoid.

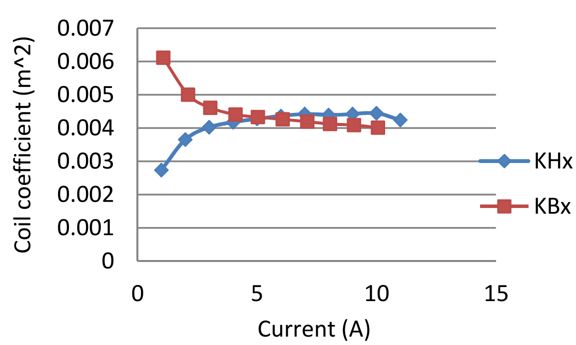

Fig. 8. The coil coefficients of B and H sensing coils.

The results from Fig. 8 are averaged over a number of measurements as K_{Hx} = 0.004241 and K_{Bx} = 0.004344.

The calibration process is important in order to eliminate the system errors before being employed to measure the magnetic field components in the 3-D magnetic properties testing system. Fig. 9 shows the photo of calibrating, and Fig. 10 plots the induced voltages in the sensing coils with different excitation currents. Fig. 11 shows the block diagram in LabVIEW for acquiring the induced voltage signals during the calibration process.

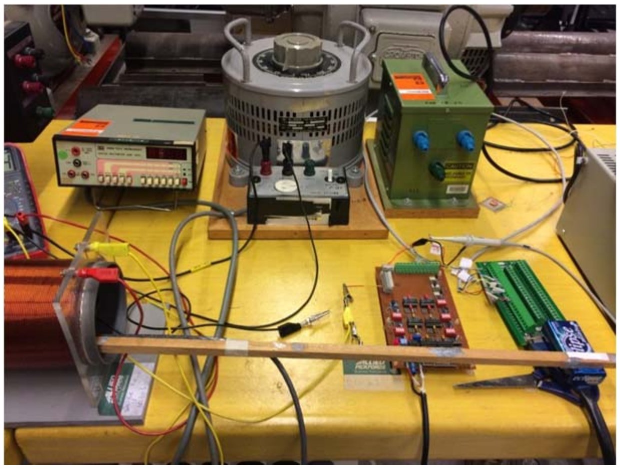

Fig. 9. Experiment of sensing coil calibration.

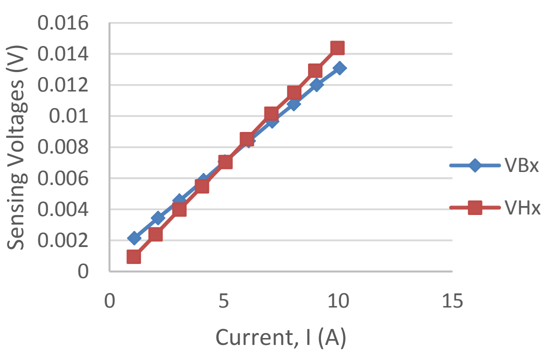

Fig. 10. The induced voltages of B and H coils during the calibration process.

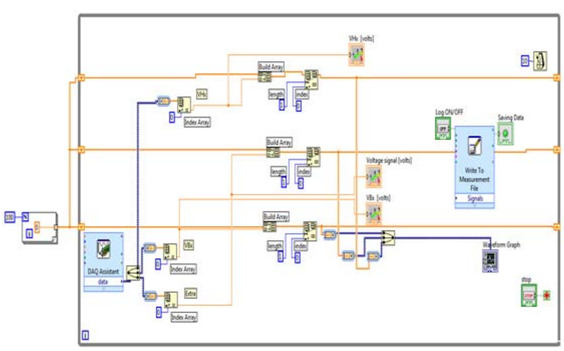

Fig. 11. Block diagram for acquiring the sensing coil voltages during the calibration.

III. Measurement

A. *Waveform Control*

As shown in Fig. 12, the waveform of excitation voltage is generated by the function generator, and exported to the channel of linear power amplifier, which feeds the excitation windings of the tester. The voltage signals of B and H are amplified by operational amplifier before having been sent to the A/D and D/A board for the data acquisition process. The signals are used to determine the relationship of *B* and *H* in order to calculate the core loss of the sample. Fig. 13 illustrates the block diagram of LabVIEW in controlling the magnetic flux density (magnitude and shape) and the data acquisition of sensing voltages of B and H coils.

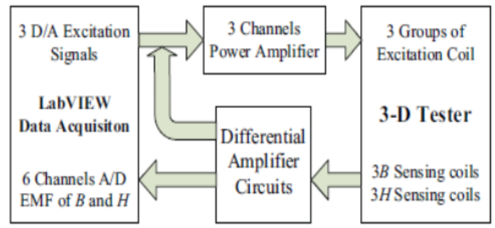

Fig. 12. Flow chart of the 3-D magnetic property testing system under 3 magnetic fluxes of excitation [2].

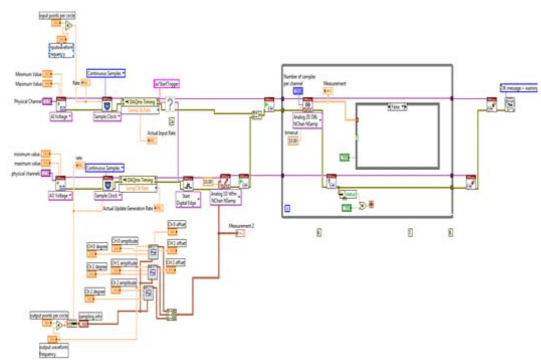

Fig. 13. Process of controlling magnetic field and acquiring the signal voltages.

The recorded data will be analyzed by Mathcad software in obtaining the important parameters such as magnetic flux density B and magnetic field strength H, in order to determine the hysteresis loop of material.

B. *Core Loss*

The core loss is calculated from the magnetic field strength H, at the sample surface and the magnetic flux density B, inside the sample, by using the field-metric method [7]. This method evaluates the total specific core loss P_t, by using the Poynting's theorem:

$$P_t = \frac{1}{T\rho_m}\int_0^T \left(H.\frac{dB}{dt}\right) dt \qquad (5)$$

where T is the time period of magnetization, ρ_m is the mass density of sample.

C. *Experimental Measurement*

The experiment at 50 Hz has been carried out by using the 3-D tester under *x*-axis penetration of magnetic flux density. The hysteresis loops for a number of increasing excitation currents of the SOMALOY 700 sample are narrower compared to that of SOMALOY 500 sample. Since the area of hysteresis loop is proportional to the core loss, the energy dissipation of SOMALOY 700 is lower than SOMALOY 500; this makes it more preferable for electrical machine application. Fig. 14 shows the hysteresis loops of SOMALOY 500 material [6], and Fig. 15 shows the measured hysteresis loops of SOMALOY 700.

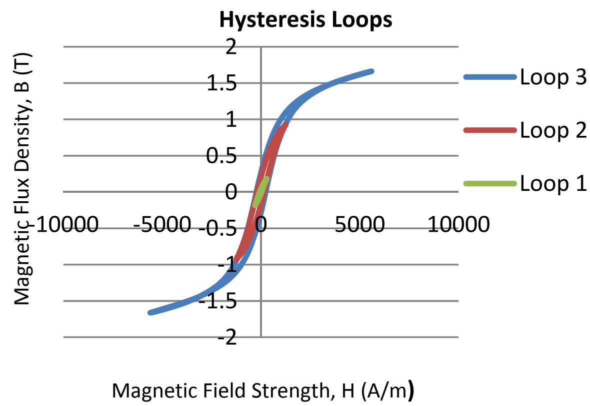

Fig. 14. The hysteresis loops of SOMALOY 500 under *x*-axis at 50 Hz of penetration.

Fig. 16 illustrates the core loss curves of two different materials, SOMALOY 500 and SOMALOY 700. The core losses of SOMALOY 700 are lower than SOMALOY 500 due to the special characteristics of SOMALOY 700, such as the new coating concept which is larger grain with ultra-high insulation [21]. During the manufacturing process, the electrical resistivity is controlled to minimize bulk eddy current losses. It also significantly reduces the hysteresis loss.

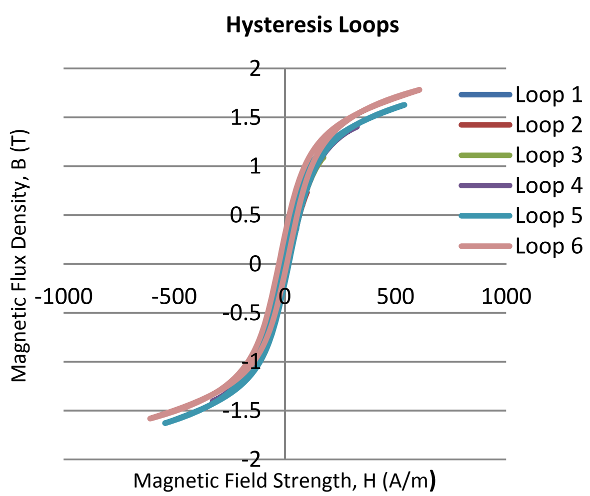

Fig. 15. The hysteresis loops of SOMALOY 700 under *x*-axis at 50 Hz of penetration.

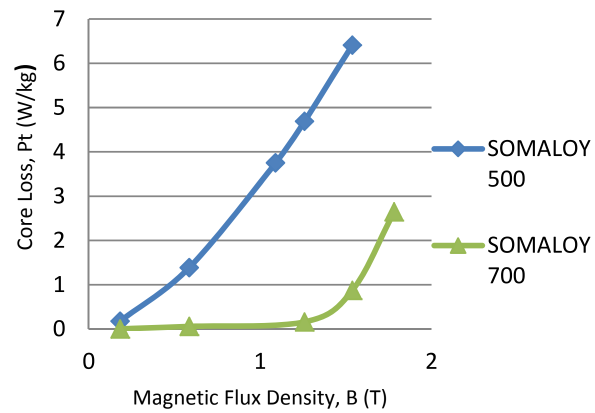

Fig. 16. The core loss of two SMC materials under *x*-axis at 50 Hz of penetration.

IV. CONCLUSIONS

This paper studies the magnetic properties measurement of new SMC product which is SOMALOY 700 (5P). It describes that area of hysteresis loops of this material are narrower than SOMALOY 500 material which corresponds to the lower core losses.

Due to the lower core loss, the power dissipation will be reduced successfully. Hence, this material is more suitable to be used in the electrical machine devices since core loss is an energy waste. This waste occurs when the power is dissipated in the form of heat within the core of electromagnetic devices due to the changing of magnetic flux field [22].

In this paper, only the 1-D measurements of SOMALOY 700 are reported. In the near future, 2-D and 3-D measurements will be investigated under rotating magnetic flux excitation.

ACKNOWLEDGMENT

The authors thank Hoganas AB for preparing the cubic sample of SMC SOMALOY 700 (5P) according to the measurement requirement.

REFERENCES

[1] Y. G. Guo and J. G. Zhu, "Applications of soft magnetic composite materials in electrical machines, a review," *Australian J. Elec. & Electron. Eng.*, vol. 3, no. 1, pp. 37-46, 2006.
[2] J. G. Zhu, J. J. Zhong, Z. W. Lin, and J. D. Sievert, "Measurement of core losses with 3D magnetic fluxes," *IEEE Trans. Magn.*, vol. 39, pp. 3429-3431, 2003.
[3] Y. J. Li, J. G. Zhu, Q. X. Yang, J. F. Sun, Y. Wang, and W. Xu, "Analysis of the 3-D magnetic reluctivity tensor based on magnetic properties measurement of SMC materials," in *Proc. Int. Conf. Electrical Machines and Systems*, 2010, pp. 1767-1772.
[4] Y. J. Li, Q. X. Yang, Y. H. Wang, J. F. Sun, J. G. Zhu, Y. G. Guo, Z. W. Lin, W. Xu, and Y. Wang, "Improved measurement of three-dimensional magnetic properties of SMC material," in *Proc. Int. Conf. Applied Superconductivity and Electromagnetic Devices*, 2009, pp. 155-158.
[5] Y. J. Li, J. G. Zhu, Q. X. Yang, Z. W. Lin, Y. G. Guo, and Y. Wang, "Measurement of soft magnetic composite material using an improved 3D tester with flexible excitation coils and

novel sensing coils," *IEEE Tran. Magn.*, vol. 46, no. 6, pp. 1971-1974, June 2010.

[6] Y. J. Li, J. G. Zhu, Q. X. Yang, Z. W. Lin, W. Xu, and Y. Wang, "Magnetic properties measurement of soft magnetic composite materials over wide range of excitation frequency," in *Proc. IEEE Energy Convers. Congress and Expo*., 2010, pp. 2259-2265.

[7] J. J. Zhong and J. G. Zhu, "Electromagnetic design of a 3D tester for magnetic properties of soft magnetic materials," in *Proc. 5th Int. Conf. Elec. Machines Syst.*, 2001, pp. 392 -395.

[8] Y. G. Guo, J. G. Zhu, Z. W. Lin, and J. J. Zhong, "Measurement and modeling of core losses of soft magnetic composites under 3D magnetic excitations in rotating motors," *IEEE Trans. Magn.,* vol. 41, no. 10, pp. 3925-3927, Oct. 2005.

[9] J. J. Zhong, J. G. Zhu, Z. W. Lin, Y. G. Guo, and J. D. Sievert, "Improved measurement of magnetic properties with 3D magnetic fluxes," *J. Magnetism and Magnetic Materials*, vol. 291, pp. 1567-1570, Apr. 2005.

[10] Z. W. Lin, J. G. Zhu, Y. G. Guo, X. L. Wang, and S. Y. Ding, "Three-dimensional hysteresis of soft magnetic composite," *J. Applied Physics*, vol. 99, no. 8, article 08D909, Apr. 2006.

[11] Y. G. Guo, J. G. Zhu, Z. W. Lin, and J. J. Zhong, "3D vector magnetic properties of soft magnetic composite material," *J. Magnetism and Magnetic Materials*, vol. 302, no. 2, pp. 511-516, Jul. 2006.

[12] Z. W. Lin, J. G. Zhu, Y. G. Guo, J. J. Zhong, and S. H. Wang, "Magnetic properties of soft magnetic composites under three dimensional excitations," *Int. J. Applied Electromagnetics and Mechanics*, vol. 25, pp. 237-241, 2007.

[13] Y. G. Guo, J. G. Zhu, Z. W. Lin, J. J. Zhong, H. Y. Lu, and S. H. Wang, "Determination of 3-D magnetic reluctivity tensor of soft magnetic composite materials," *J. Magnetism and Magnetic Materials*, vol. 312, pp. 458-463, May 2007.

[14] J. G. Zhu, Z. W. Lin, Y. G. Guo, and Y. K. Huang, "3D measurement and modelling of magnetic properties of soft magnetic composite," *Przeglad Elektrotechniczny (Electrical Review)*, vol. 85, no. 1, pp. 11-15, Jan. 2009.

[15] Y. J. Li, J. G. Zhu, Q. X. Yang, Z. W. Lin, Y. G. Guo, and Y. Wang, "Measurement of soft magnetic composite material using an improved 3D tester with flexible excitation coils and novel sensing coils," *IEEE Tran. Magn.*, vol. 46, no. 6, pp. 1971-1974, June 2010.

[16] Y. J. Li, Z. W. Lin, H. X. Liu, Y. Wang, Y. G. Guo, J. G. Zhu, and Q. X. Yang, "Three-dimensional magnetic properties of soft magnetic composite material at different frequencies," *J. Applied Physics*, vol. 109, no. 7, article P07B503, 2011.

[17] Y. J. Li, J. G. Zhu, Q. X. Yang, Z. W. Lin, Y. G. Guo, and C. Zhang, "Study on rotational hysteresis and core loss under three-dimensional magnetization," *IEEE Trans. Magn.*, vol. 47, no. 10, pp. 3520-2523, 2011.

[18] Y. J. Li, Q. X. Yang, J. G. Zhu, and Y. G. Guo, "Magnetic properties measurement of soft magnetic composite materials over wide range of excitation frequency," *IEEE Trans. Ind. Applicat.*, vol. 48, no. 1, pp. 88-97, 2012.

[19] A. R. Asari, Y. G. Guo, J. G. Zhu, and F. Ismail, "A review on 3-D magnetic property testing system for measuring rotational core loss of soft magnetic materials," in *Proc. 10th Asian Control Conf.*, 2015, pp. 294-299.

[20] Y. G. Guo, J. G. Zhu, Z. W. Lin, J. J. Zhong, H. Y. Lu, and S. H. Wang, "Calibration of sensing coils of a three-dimensional magnetic property tester," *IEEE Trans. Magn.*, vol. 42, pp. 3243-3245, 2006.

[21] SGTechnologies Delivering Performance, *Soft Magnetic Composite*, https://www.sgtec.com/materials/soft-magnetic-components-smc. Accessed on July 4, 2015.

[22] AK Steel, *Selection of Electrical Steels for Magnetic cores*, 2007, Retrieved from www.aksteel.com on April 4, 2012.